



Research Article

Numerical and experimental study on the collector and chimney modifications of a solar chimney power plant

Rajamurugu NATARAJAN^{1,*}, Akhil Chandramohanan Kumari SUNI²,
Likhith Raj PEDASINGU², Yaknesh SAMPATH³

¹Department of Aeronautical and Aerospace Engineering, KCG College of Technology, Chennai, 600 097, India

²Department of Aeronautical Engineering, Bharath Institute of Higher Education and Research, Chennai, 600 073, India

³Department of Aerospace Engineering, Chandigarh University, Punjab, 140413, India

ARTICLE INFO

Article history

Received: 10 July 2023

Revised: 15 December 2023

Accepted: 16 December 2023

Keywords:

C-D Chimney; Generation
Renewable Energy; Green
Technology; Solar Chimney;
Solar Power

ABSTRACT

The environmental hazard posed by global warming necessitates the development of sustainable, eco-friendly power production unit based on renewable energy principles. Solar Chimney Power Plants (SCPP) are the resource that fits this description. Here, the chimney is equipped with a larger roof at bottom, referred as collector, absorbs the sunlight to warm the air inside. This heat creates an upward draft, resulting a forward motion of air, which rotates the turbine. There is a better possibility of enhancing the performance of an SCPP with modification of factors such as chimney height, collector area, collector angular position. Hence, this research objective is to study the alteration in efficiency of an SCPP with collector angular modifications, such as completely slopped, intermediately sloped profiles, as well as the effects of various chimney designs with area ratios larger than one. An additional study of a semi divergent (SD) chimney with a completely slanted collector, positioned vertically. Initial analysis is performed using ANSYS-FLUENT, and a simulation environment is modeled to mimic the various chimney and collector configurations in preparation for the experimental work. The better model is chosen from these simulations and experimented in true environmental conditions. It was determined that the average increase in temperature within the SCPP was 17 K. The research found that the collector setup with a slope of 50% (case-2) resulted in a peak velocity 12% higher than that of the fully sloped configuration (case-1). Additionally, case-2 was 23% more productive than the Manzanares facility. On the other hand, case-3's semi divergent chimney with a complete slopped collector outperformed the other two by 23% and 12%, respectively.

Cite this article as: Natarajan R, Suni ACK, Pedasingu LR, Sampath Y. Numerical and experimental study on the collector and chimney modifications of a solar chimney power plant. J Ther Eng 2024;10(6):1539–1558.

*Corresponding author.

*E-mail address: n.rajamurugu@gmail.com

This paper was recommended for publication in revised form by
Editor-in-Chief Ahmet Selim Dalkılıç



INTRODUCTION

At present, the enhanced accumulation of CO₂ emission in developing countries poses a significant threat to the environment. Therefore, it is imperative for nations to adopt a concrete and decisive approach to mitigate the depletion of fossil fuels and the overexploitation of natural resources in power production. Renewable energy sources are widely acknowledged as a promising solution for the entire production of global electricity in near future. SCPP is a viable technology suitable not only for energy production, also in natural ventilation for buildings, crop humidifying in arid regions, and desalination of seawater. The fundamental principle of a solar chimney associates with variation of density in the region behind collector, results the propulsion of air in an upward direction with increase in momentum of the flow from inlet to outlet sections of chimney. solar chimney mainly consists of components such as transparent collector, here there is a solar energy refraction essential to enhance the air temperature; long slender like structure called chimney which drives the hot air to rise upward due to updraft effect. Turbines are placed either inside the chimney or may be placed at the collector chimney junction which is rotated due the momentum increment in upward motion of hot air. Thus, an appropriate mechanism must be provided to transform the turbine's kinetic energy into electrical energy. The first pilot SCPP proposed by Prof. Schlaich, constructed in 1982 at Manzanares, Spain to generate 50MW under full load condition (Das P and Chandramohan 2022). Numerous previous studies have aimed to explore the SCPP efficiency. The main focus of this study is about investigating the effect of geometric factors on solar chimney performance through numerical, experimental approach. The manuscript is organized into four sections. The first section provides a literature review and discusses empirical relationships. Section 2 presents computational studies, while section 3 reports the experimental findings and comprehensive summary of the study's key observations and also discusses the environmental impact of the proposed research in detail.

Literature Survey

Extensive investigations have been initiated by various scholars in the aspect of utilization of an SCPP as a prominent energy source. Das and Chandramohan [1] critically examined on this area with a particular focus on environmental and geometric parameters, barriers to commercialization, opportunities, and carbon emission reduction. They emphasized the importance of these parameters in solar chimney design, optimization, and the capability of SCPP in mitigating carbon emission. Vakili and Salehi [2] conducted a review on the implementation of machine learning techniques to model solar collectors, by discussing algorithms such as artificial neural network, support vector machines, and decision trees. They highlighted the potential of machine learning in improving the accuracy and efficiency of collector modeling. Mehta et al. [3]

focused on advancements in mixed-mode solar thermal dryers, reviewing techniques to enhance the performance, efficiency, and reliability. Purnachandrakumar et al. [4] explored importance of the computational fluid dynamics (CFD) for evaluating the performance of solar stills in water desalination. They discussed the impact of CFD simulations on optimizing parameters such as temperature distribution, evaporation rates, and overall efficiency. Mehranfar et al. [5] comparatively analyzed on the methodology of enhancing the efficiency, including solar tracking, energy recovery, and thermal storage. They discussed the advantages and challenges associated with each method. These studies provide valuable insights to enhance SCPP performance. The previous research reviews are categorized into three sections in this study: computational/analytical studies, experimental studies, and modern applications of SCPP.

Literatures Pertaining to Computational Studies/Analytical Studies

Das and Chandramohan [6] utilized computational fluid dynamics (CFD) to analyze the influence of numerous geometric configurations on solar updraft tower (SUT) performance. They investigated on height of the chimney, diameter of absorber plate, and collector roof inclination angle. In another study, Das and Chandramohan [7] conducted CFD simulations to analyze the effect of design parameters on flow parameters, SUT performance. Gholamalizadeh and Kim [8] employed a two-band radiation model in CFD analysis for the investigation of greenhouse phenomenon in solar chimney. Hooi and Thangavelu [9] conducted parametric simulations using CFD to examine the performance of an SCPP under different operating circumstances. Amudam and Chandramohan [10] accomplished a numerical study to estimate the SUT performance, considering factors such as the chimney angular divergence and ambient temperature. Balijepalli et al. [11] used CFD simulations to explore the performance characteristics of a lab-scale SUT, by concentrating on geometric configurations. Chitsomboon [12] furnished an analytical model to examine solar chimney air flow. Koonsrisuk [13] originated a mathematical model and compared the conventional, sloped profiles of SCPP. Koonsrisuk [14] focused on the sloped solar chimney mathematical modeling. Koonsrisuk and Chitsomboon [15] studied the impact of flow area variation in a solar chimney. Koonsrisuk and Chitsomboon [16] advanced a single non-dimensional variable for solar chimney modeling. Koonsrisuk and Chitsomboon [17] compared conventional, sloped models with analysis of second law. Ayadi et al. [18] investigated on the impact of turbine blade number in airflow inside solar chimney. Fei Cao et al. [19] analyzed the variation in solar chimney performance for conventional, sloped constraints at different locations of China. Koonsrisuk et al. [20] proposed a design configuration based on constructal design principles. Zhou et al. [21] numerically examined the compressible flow inside a solar tower with an appropriate

chimney geometric height analysis. Ming et al. [22] studied the air flow, heat transfer characteristics inside a solar chimney profile installed with thermal storage bed. Keshari et al. [23] performed a numerical evaluation to validate the optimum collector inclination angle of a solar updraft tower. Sundararaj et al. [24] conducted a study of parametric optimization based on response surface methodology to enhance to validate the quality of resultant data in SCPP analysis. These studies offer the important characteristics to optimize the solar tower, collector roof design parameters to achieve an improved performance with a better advancement of efficiency in overall power plant.

Literatures Pertaining to Experimental Studies

Ghulamchi et al. [25] conducted experiments to examine the impact of geometrical variation, climatic fluctuation on scaled-solar tower model performance. They analyzed on air velocity, temperature distribution, and power generation for validating geometry and climatic influence on system's efficiency. This study provided valuable insights in optimizing the design of an SCPP in small-scale perspective. Gannon and von Backstrom [26] conducted a cyclic investigation on the solar tower system, by considering the system losses, solar collector performance. They examined various losses within the system and the collector's performance to evaluate the overall efficiency. Guo et al. [27] implemented an analysis for the influence of heat storage system on solar chimney performance. They investigated on following parameters, heat storage material, capacity, and discharge efficiency to evaluate system's ability of storage with proper emission of thermal energy. Koonsrisuk and Chitsomboon [28] assessed the theoretical model preciseness in predicting the performance. They compared the predictions of different models with experimental data to determine their accuracy. Mehdi-pour et al. [29] initiated an investigation through experimental implementation for estimating the capability of an energy tower and evaluated the importance of tower height, sun radiation, humidity on its overall efficiency. The study aimed to understand the importance of these factors influence in energy tower's performance. Ridwan et al. [30] presented a design and experimental test of an SCPP based on a case study in Indonesia. They constructed a small-scale prototype and conducted field measurements to evaluate its performance. Okada et al. [31] proposed an advancement in power generation by incorporating a diffuser tower in solar chimney design. They investigated on usage of a diffuser tower to achieve a qualitative improvement in output power performance of this system. Natarajan et al. [32] conducted relative investigations on the solar tower capability with scale ratio variants. They investigated about scale ratio necessity on performance parameters of solar towers using numerical simulations. Zhou and Yang [33] analyzed the solar collector temperature distribution field, along the exploration on potential feasibility of SCPP in China. Zhou et al. [34] undertaken an experimental approach on temperature

distribution inside the solar chimney system. Kassaei et al. [35] investigated the feasibilities of solar chimney system for natural ventilation in residential applications. They reviewed the literature specified the solar chimney application as a natural ventilator in household premises including analysis of its performance and effectiveness. These studies collectively contribute to the understanding of SCPP principles, idealizing aspects such as geometry optimization, cyclic analysis, heat storage performance, accuracy of theoretical models, environmental factors, experimental assessments, diffuser tower utilization, scale ratios, temperature field analysis, and natural ventilation applications. Ikhlef et al. [36] investigated the effect of different environmental conditions on small and large prototype SCPP's. The investigation found that the region of high wind velocity shown a decrease in power production.

Literatures Pertaining to Applications Of SCPP

Chitsomboon [37] investigated on the feasibility of a solar chimney to function as a better renewable energy technology for generating electricity by discussing its potential and efficiency. Ferreira et al. [38] evaluated about technical application of solar chimney as a humidifier to dry the required food materials, analyzing factors such as airflow patterns, temperature distribution, and drying efficiency. Das and Chandramohan [39] conducted numerical studies on a solar vortex engine to understand the variation in its flow parameters along power potential, optimizing its geometric configurations. Rao and Sivalingam [40] assessed an evacuated tube solar dryer's energy, exergy, environmental, and economic aspects for drying agricultural products. Muthu and Ramadas [41] experimentally investigated on the bifacial solar module performance, analyzing energy production, exergy efficiency, economic feasibility, and environmental impact. Nazari and Daghigh [42] has investigated about feasibility of a solar still with boxed configuration, cover less, equipped with thermoelectric condensing duct to examine the temperature of components, period of energy payback, distilled water production quality, water hygiene approximation. They concluded that, presence of a dish concentrator in a boxed parabolic profile with their still configuration in terms of exergo enviro economic can maintain a better financial reserve. Sadeghi and Nazari [43] investigated on a hybrid nanofluid with an antibacterial property, to sterilize the potable water by capturing its magnetic properties to increase the heat transfer rate in a sloped solar still system equipped evacuated tube collector, thermoelectric channel. These studies contribute to understand the applications and performance of solar chimneys in electricity generation, food drying, water heating, solar stills, enhanced efficiency methods, agricultural drying, and vertical bifacial solar modules. Phu et al. [44] introduced V-cap to induce vortex in the direction of chimney and enhanced the mass flow rate. This study seems to be interesting in the aerodynamic study of the solar chimneys.

Research Gap

The present study addresses the research gap by investigating the effectiveness of different collector configurations and chimney designs in SCPPs. Previous studies have mainly focused on evaluating performance, efficiency, and numerical simulations, while the main aspect is, exploration of the influence of specific variables for designed SCPP models such as impact of various collector configurations, including completely sloped and intermediately sloped collectors, on the performance. Also, investigates the effects of different chimney designs, particularly the Semi Divergent (S-D) chimney with a completely slanted collector.

Objective

In this study, the computational and experimental approach on different collector and chimney configurations are presented in a precise manner. Every geometrical change sought to the conventional SCPP is presented with simulation and experimental results. This study presents three experimental studies, aimed at gaining a comprehensive understanding of the influence of collector, chimney area ratios. The experiments were conducted to investigate the relationship between these variables and their effect on the overall performance of the system.

Numerical Modelling

The basic form of fundamental equation linking to the efficiency of all system components is given by Zhou et al. [45]. Power output parameter, P of a solar tower is represented in equation 1-3.

$$\text{PowerOutput}(P) = q_{solar} * \eta_{coll} * \eta_{tur} * \eta_{tower} \quad (1)$$

$$q_{solar} = GA_{col} \quad (2)$$

$$\eta_{tower} = \frac{P}{q} \quad (3)$$

Fluid flow power has a direct proportionality with pressure drop or tower driving potential. The Flow power can be expressed by equation 4.

$$p = \Delta p(V_{max})(A_{col}) \quad (4)$$

$$\Delta p = (\rho_{atm} - \rho_{tower})gH \quad (5)$$

The difference in buoyancy of heated air is proportional with change in pressure inside tower geometry, which is given by equation 5. Pressure difference inside the chimney is generated by the air passage to advance in a forward direction.

The loss of air flow velocity inside the chimney is negligible in the case of absence of a turbine. Equation to calculate pressure fluctuations in the tower is denoted as equation 6. The velocity can be determined by equation 7.

$$P = \frac{1}{2} m V_{max}^2 \quad (6)$$

$$V_{max} = \sqrt{2gH \frac{(\rho_{atm} - \rho_{tower})}{\rho}} \quad (7)$$

The maximum velocity equation can be simplified further by boussinesq approximation (equation 8). Tower efficiency relation is described in equation 9.

$$V_{max} = \sqrt{2gH \frac{(\Delta T)}{T_o}} \quad (8)$$

$$\eta_{tower} = \frac{gH}{C_p T_o} \quad (9)$$

The maximum updraft velocity (Equation 8) is observed near the solar tower base. Hence a turbine can be typically positioned here. Chimney efficiency is primarily determined by its height, as illustrated by Equation (10), which provides a simplified representation of this characteristic. The Boussinesq approximation's deviation from the precise solution is negligible at heights above 1000 m. As a consequence, improving tower efficiency may be done by altering the collector angle, employing various diffuser types in the chimney section, and figuring out the best turbine location. Mass flow rate inside the chimney can be evaluated with the product of specific parameters, velocity, density, collector area as expressed in equation 10.

$$\dot{m} = \rho A_{coll} V = \rho \pi r^2 \sqrt{2gH \frac{(\Delta T)}{T_o}} \quad (10)$$

Therefore, it is essential to conduct a comprehensive investigation into the optimized chimney diameter, collector diameter, and collector inclination angle. As depicted in Figure 1, V_1 is the velocity of inlet airflow from ambient to collector, V_3 is the exit velocity of the air flow from diverging chimney to ambient atmosphere contributes to the efficiency equation of the tower. The heat absorbed by ground

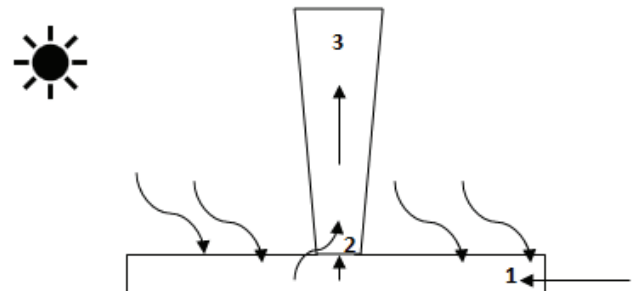


Figure 1. Chimney – divergent model.

is uniform across the plane, is an assumption, and enhancement in surrounding air temperature leads to steady-state temperature of collector profile.

Equation 11 describes the velocity of the fluid flow as it exits chimney inlet/base region, including temperature difference, corresponding rise in kinetic energy. Additionally, equations 12 to 14 provide further expressions related to this phenomenon.

$$V_2 = \sqrt{2gh \frac{\Delta T}{T}} \quad (11)$$

$$\frac{1}{2} \dot{m} V_3^2 = \dot{m} C_p \Delta T' \quad (12)$$

$$V_3^2 = \sqrt{2C_p \Delta T'} \quad (13)$$

$$V_2 = \frac{A_3}{A_2} V_3 \quad (14)$$

Buoyancy effect, kinetic energy transferred to turbine implements a temperature rise at the chimney outlet. Equation 15 quantifies the relevant energy output, while the efficiency of the system can be estimated from equations 16 to 18.

$$GA_{coll} = \rho A_2 V_2 C_p (\Delta T + \Delta T') \quad (15)$$

$$\eta = \frac{\Delta T'}{\Delta T + \Delta T'} = \frac{\frac{v_3^2}{2C_p}}{T \left(\frac{A_1}{A_2}\right)^2 \left[\frac{v_2^2}{2gh} + \frac{v_2^2}{2C_p}\right]} \quad (16)$$

$$TC_p \gg gh \left(\frac{A_3}{A_2}\right)^2 \quad (17)$$

$$\eta = \frac{gh}{TC_p} \left(\frac{A_3}{A_2}\right)^2 = \frac{gh}{TC_p} \left(\frac{\text{chimneytoparea}}{\text{chimneybasearea}}\right)^2 \quad (18)$$

A dimensionless variable is framed for the power plant operated on solar power by Chitsomboon, Koonsrisuk [17, 18] given in equation 19. The power induced and efficiency was expressed by equation 20 and 21.

$$\frac{\rho A V \frac{V^2}{2}}{\frac{q' A_r \beta}{C_p} gh_c} = 1 \quad (19)$$

$$\frac{1}{2} \dot{m} * (V_{max})^2 = \frac{q' A_r \beta}{C_p} gh_c \quad (20)$$

$$\eta_{tower} = \frac{\beta gh_c}{C_p} \quad (21)$$

Solar chimney efficiency can be determined by the equation 1/T for a perfect gas. It is directly influenced by the geometric chimney height parameter, had an inverse relation with collector intake temperature, and unaffected with temperature rise associated in collector. To enhance the efficiency along with maximum power extraction from turbine rotation, adjusting collector and chimney geometric profiles, as well as applying the improved flow characteristics are considered the most straightforward approach. While numerous research has been concentrated on the impact of altering the chimney shapes, including cylindrical, convergent, or divergent. The findings have remained ambiguous throughout the time. Divergent type solar chimneys, though, can increase effectiveness, according to current studies. Airflow inside the SCPP region from collector inlet to chimney outlet/top is driven by the driving potential, denoted as “ Δp ”, defined by the difference in between atmospheric pressure to the static pressure of the heated airstream at chimney base [46]. Equation 22 represents the driving potential inside the system.

$$\Delta p = (\rho_o - \rho)gH_{chim} + 0.5\rho V_2^2 \left[1 - \frac{A_3^2}{A_2^2}\right] \quad (22)$$

For a straight cylindrical chimney with similar area of cross section at chimney end (A3), at collector intersection (A2), the equation mentioned earlier remains the same. In this case, obtained output power is controlled by volumetric air flow rate and turbine pressure drop. Potential power generation of SCPP is estimated in this study, using a 2D model that does not include a genuine wind turbine but does include a separate pressure drop model as shown in equation 23 [46].

$$P_{out} = y \times \Delta P_{tot} \times V_t \times A_{coll} \quad (23)$$

Variable “y” represents the ratio of turbine pressure drop to overall driving potential. According to (Gannon et al. 2003), the maximum potential pressure drop in a constant-driving-potential system is $x = 2/3$. However, few studies have shown that the ideal power output may be underestimated by this factor (Zhou et al. 2009). The research discusses the theoretical development of a prototype for divergent solar chimneys. It demonstrates the ratio of solar energy converted to kinetic energy of airflow at chimney base is proportional to $(A_3/A_2)^2$, here A3 represents the cross-sectional area of the chimney top and A2 represents the area of the chimney base. If A3 equates to A2, equation 18 corresponds to Zhou et al.’s [21] solar chimney with a cylindrical cross-section. Additionally, the diverging solar chimney efficiency increases with $(A_3/A_2)^2$. These findings align with the conclusions drawn by Koonsrisuk and Chitsomboon [28], as confirmed by equation (21). In a condition, when chimney area of the base A2 is less than

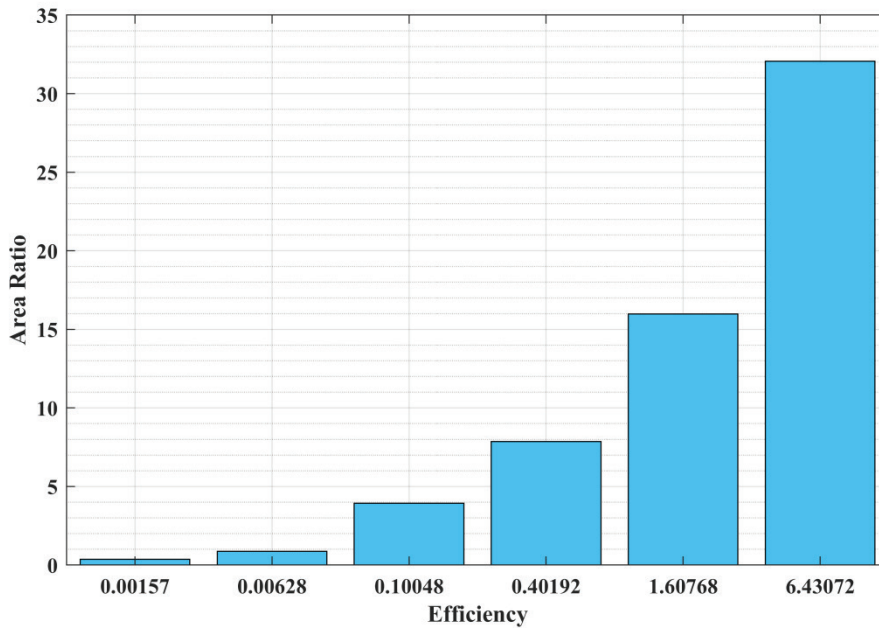


Figure 2. Constant height of 195 m - area ratio vs. efficiency.

top area A_3 , the system's efficiency rises, resulting under-expanded chimneys. Figure 2 depicts a comparison of the efficiencies according to Equation (18). As a result, when $A_3 > A_2$, divergent chimney outperformed typical straight chimney. But if $A_3 = A_2$, system performance is similarly to previous systems (Over Expanded Chimneys), however this system outperforms both conventional, diverging chimney profiles in terms of pressure drop. When A_3/A_2 ratio approaches greater values, such as 16 and 32, the system's efficiency rises dramatically, but the building of such towers is impractical due to the intricacy of the design. From this mathematical approach, it is concluded that divergent chimney profile is more efficient than with conventional/cylindrical chimney profiles.

Problem Statement

In this study there are three types of chimneys considered for analysis, depicted in Figure 3. The experimental setup has a chimney height of 2m with collector radius,

2.4m for all the three cases. Here, the completely slopped collector is equipped to first model (Figure 3 (case-1)) and second has an intermediate slopped collector, where half the collector is parallel to ground, while portion is inclined as shown in Figure 3 (case-2). Final model has a chimney modification; half the portion is linear and remaining is diverging exactly at its middle (ie., 1 m) from the base as shown in Figure 3 (case-3) with completely slopped collector. The flow properties inside the chimneys are analyzed using computational and experimental techniques.

Computational Studies

In this study, the flow characteristics within the solar chimney were analyzed by solving the Navier-Stokes equations using Ansys-Fluent 2021R2. K-epsilon method was employed to study turbulence in the constructed solar chimney power plant models. Several flow assumptions were made, including steady three-dimensional turbulent flow, axisymmetric flow regime, and fluid binding with

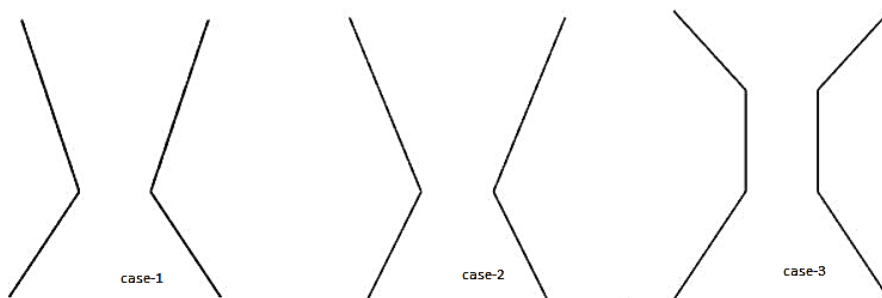


Figure 3. Solar chimney structures considered for study.

Boussinesq Approximation. The model was appropriately meshed for the simulation. Prepared mesh models were imported to Fluent setup solver. Proper boundary conditions were set up for the imported model, with gravity defined as 9.81 m/s² along negative Z-axis in typical configuration. The radiation affected by models were represented with Discrete Ordinates (DO) system. Solid zone contributed to radiation is defined as a transparent medium as existed in boundary conditions. Solar tracking was incorporated in the model to account for the varying radiation intensity across the chimney area. The buoyancy Rayleigh number (Ra) were adopted to define the flow properties, to determine the presence of natural convection and its intensity. If the Ra number exceeded 109, turbulence was observed within the solar chimney. For analyzing the flow characteristics, the k-epsilon two-equation viscous model, suggested by Ming et al. [22] were implemented, and RNG model was for analyzing the turbulent condition. The governing equations of the simulation, as provided by Hu et al. [46], included the continuity equation (24), momentum equation (25), energy equation (26), k-epsilon equations (27), and their balance equations (28-31).

$$\frac{\partial(\rho u)}{\partial t} + \nabla \cdot \rho \vec{V} = 0 \quad (24)$$

$$\rho \left[\frac{\partial \vec{v}}{\partial t} + \vec{v} \cdot \nabla \vec{v} \right] = -\nabla p + \mu \nabla^2 \vec{v} + \frac{1}{3} \mu \nabla (\nabla \cdot \vec{v}) + \vec{F}_b \quad (25)$$

$$\frac{\partial}{\partial t} (\rho k) + \frac{\partial}{\partial x_j} (\rho k u_j) = \frac{\partial}{\partial x_j} \left[\left(\mu + \frac{\mu_t}{\sigma_k} \right) \frac{\partial k}{\partial x_j} \right] + G_k + G_b - \rho \epsilon - Y_M + S_k \quad (26)$$

$$\frac{\partial}{\partial t} (\rho \epsilon) + \frac{\partial}{\partial x_j} (\rho \epsilon u_j) = \frac{\partial}{\partial x_j} \left[\left(\mu + \frac{\mu_t}{\sigma_\epsilon} \right) \frac{\partial \epsilon}{\partial x_j} \right] + \rho C_1 S_\epsilon - \rho C_2 \frac{\epsilon^2}{k + \sqrt{\nu \epsilon}} + C_{1\epsilon} \frac{\epsilon}{k} C_{3\epsilon} G_b + S_\epsilon \quad (27)$$

$$C_1 = \max \left[0.43, \frac{\eta}{\eta + 5} \right] \quad (28)$$

$$\eta = S \frac{k}{\epsilon} \quad (29)$$

$$S = \sqrt{2S_{ij}S_{ij}} \quad (30)$$

Boussinesq Approximation

Simulations of this study were depended on buoyancy effect. In this approximation, air density applied in mentioned governing equations is assumed to be constant, and the body force is calculated using equation 31. The system power output is determined by equation 32.

$$(\rho - \rho_o)g = -\rho\beta(T - T_o)g \quad (31)$$

$$P_{out} = \dot{m}gH_c \frac{\Delta T}{T_a} = P_{out} = (\rho AV)gH_c \frac{\Delta T}{T_a} \quad (32)$$

Boundary Conditions

Constant values $\sigma_k, \sigma_\epsilon, C_\mu, c_1, c_2$ are employed in the k-epsilon turbulence equations. In equation (33), v, u are parallel and perpendicular flow velocity components with reference to direction of gravitational effect. In this study, the effects of gravity were considered at negative z axis, with magnitude 9.81 m/s. The models are operated at the defined pressure similar to ambient atmospheric pressure of 101325 Pa with temperature, 303 K.

$$\begin{aligned} \sigma_k &= 0.7194 \\ \sigma_\epsilon &= 0.7194 \\ C_\mu &= 0.0845 \\ c_1 &= 1.42 \\ c_2 &= 1.68 \\ c_3 &= \tan \frac{\nu}{u} \end{aligned} \quad (33)$$

This study examined the flow physics within a domain by applying boundary conditions (BCs) as similar as on actual flow possibilities. The operational conditions for cell zones were maintained at 303K, 1 atm. The BC type at inlet and outlet of designed SCPP models is a pressure inlet and pressure outlet. The collector roof was considered to be a partially transparent, it is assumed that solar flux will reduce on its surface. Here, 10W/m²K is the applied magnitude of heat transfer coefficient in the convection phenomenon. polythene is the material for collector cover.

Table 1. Boundary conditions

Name	Zone type	Thermal conditions	Boundary Condition Type
Chimney	Wall	Heat flux	Opaque
Collector	Wall	Convection	Semi-transparent
Ground	Wall	Heat flux	Opaque
Inlet	Pressure inlet	Temperature, T=303K	Pressure, p=0 pa
Outlet	Pressure outlet	Heat Flux, q=0	p=0 pa

Properties of this material were specified in the solver for the accurate approximation. Chimney boundary is defined as in similar manner with adiabatic wall properties. The chimney material is galvanized iron, polythene plastic film is collector material, and the ground is sand.

Solution Methods

The modeling and simulation were produced using CFD simulations. Using the finite volume technique (FVM), resolve governing equations including energy, momentum, and continuity. The subsequent actions were to perform out numerical simulations and to select the solver parameters.

- i) The strategy for the pressure-volume coupling solution is simple. PRESTO methodology is selected for pressure, second order upwind is employed for all the schemes other than Discrete Ordinates.
- ii) First-order upwind is employed for Discrete Ordinates. The solution is initiated and iterated with the convergence criteria set to 10^{-6} . The produced models are loaded into ANSYS ICEM - CFD for meshing.
- iii) Tetrahedral element is employed to discretize the model domain
- iv) Figure 4 is selected for model meshing in order to achieve a better outcome.

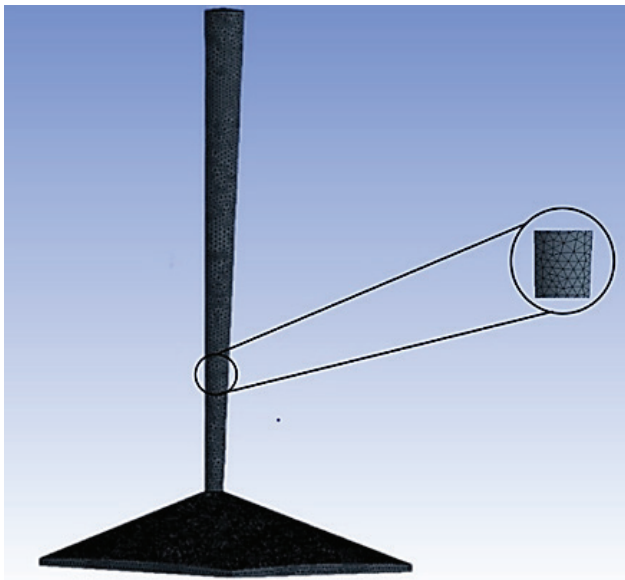


Figure 4. Case-1 Solar chimney model with mesh.

- v) All four models were created using this tetrahedral mesh, which produced a fine mesh. In the simulation process, the working fluid is air.

Initially the mesh count for Case 1 has a total number of 51,978 nodes and 269,567 elements. Case 2 is equipped with 69,479 nodes; 369,887 elements and Case 3 is with 26,855 nodes and 122,351 elements.

Grid Independence Study

Requirement of precise numerical results is mandatory for further experimentation and numerical validation in this study. Therefore, grid adaptation based on velocity gradient was employed to ensure the independence of flow parameters on mesh element number. The curve approach has been followed, where the flow is smooth, and the usual standard normalization was utilized so because residuals are not normalized. Furthermore, a refining threshold of around 25% of the grid was specified. Grid independence test is conducted on different mesh types, the resulted average velocity gradients were presented in Table 2. The individual gradient parameters were resulted with minimal deviation in all cases, specifies the performed independence study is valid.

Subsequently, numerical simulation was carried on the Manzanares solar updraft tower and resulted computational flow parameters, velocity and temperature were compared with the simulation work of Hooi and Thangavelu carried in [9], along with true Manzanares model flow parameters. This validation provides a satisfactory conclusion with minimal deviation in the maximum velocity, temperature rise. Resulted magnitude of the flow parameters were presented in Table 3. Figure 5 visualizes the air flow velocity in this model inside the Manzanares model. Maximum velocity, 14.9 m/s is generated in the region of transition which is the region of intersection of collector, chimney profiles with an increment of 18 K in temperature. Further simulations on case models in this study were conducted with similar methodology, employed to Manzanares solar updraft tower model in a consistent approach.

Experimental Studies

In this study, real-time experiments of all cases (Figure 6) were conducted on three different solar chimney power plants (SCPPs) under open atmospheric conditions. Each experiment model had an area ratio greater than unity but varied in chimney layout. The first case involved a sloped collector and a fully divergent chimney, while the second

Table 2. Results of grid independence test

Mesh Type	Number of Nodes	Number of Elements	Average Velocity (m/s)
Coarse	8994	27361	13.12131
Medium	10951	34495	13.14088
Fine	13199	43716	13.14658

Table 3. Comparison of the CFD work with existing literature

Type	Velocity (m/sec)	Rise in Temperature (K)
Manzanares	15	20
Simulation Work carried out in 2018 by Thangavelu and Hooi et. al.	15.7	21.9
Present Simulation work	14.9	18

case examined a divergent chimney placed on a semi-sloped collector to assess the collector’s impact on overall system performance. In the third case, the chimney was modified to diverge only at the top while remaining is cylindrical towards the bottom, with a completely sloped collector. Polyethene sheets were used as the collector material to refract solar energy. K-type thermocouples are used in this study for temperature measurement. Six thermocouples were used, with three positioned at distances of 8 cm, 110 cm, and 190 cm inside the chimney, and the remaining three placed at inlet, middle, and transition regions inside collector section. Velocity measurements in chimney, collector was measured with hot wire anemometer.

Uncertainty analysis for the study of input variation on output variance is performed, considering limitations of the experimental measuring devices. The hot wire anemometer used had an accuracy range of 3% to 0.1% and a measurement range of 0-50 m/s. Thermocouple had a sensitivity of

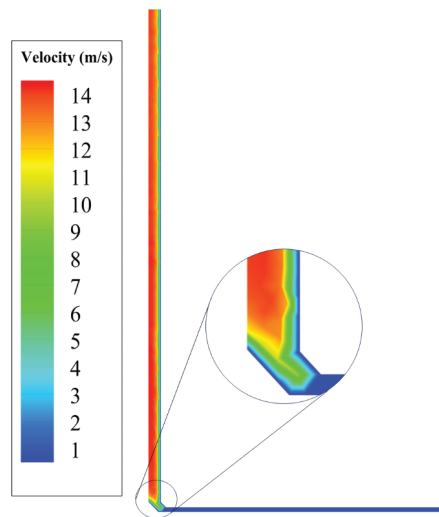


Figure 5. Manzanares solar tower (velocity contour).



Figure 6. Experimental setup of all cases.

0.006 mV/°C at 25°C, 0.013°C is the equivalent temperature uncertainty with an accuracy of 2.2°C or 0.75%. Each model was evaluated approximately for a single day, from 9:00 a.m. to 4:00 p.m., with manual temperature and velocity readings extracted for a half an hour time interval.

RESULTS AND DISCUSSION

Results from these experiments are analyzed and obtained data can be expected in the satisfactory range of providing valuable insights for better improvement in

overall effectiveness of SCPP. In an axial chimney symmetric plane, the velocity intensity distribution for case-1, 2 is depicted in Figures 7a-d. These findings reveal that peak velocity values are observed near the inlet chimney inlet. Air velocity gradually reduces along the positive y direction of chimney axis. This is attributed to the maximum driving potential being present at the chimney inlet. SA

While examining the velocity values outside the chimney, along the collector, it is observed that velocity drops significantly farther from chimney axis. Temperature contour

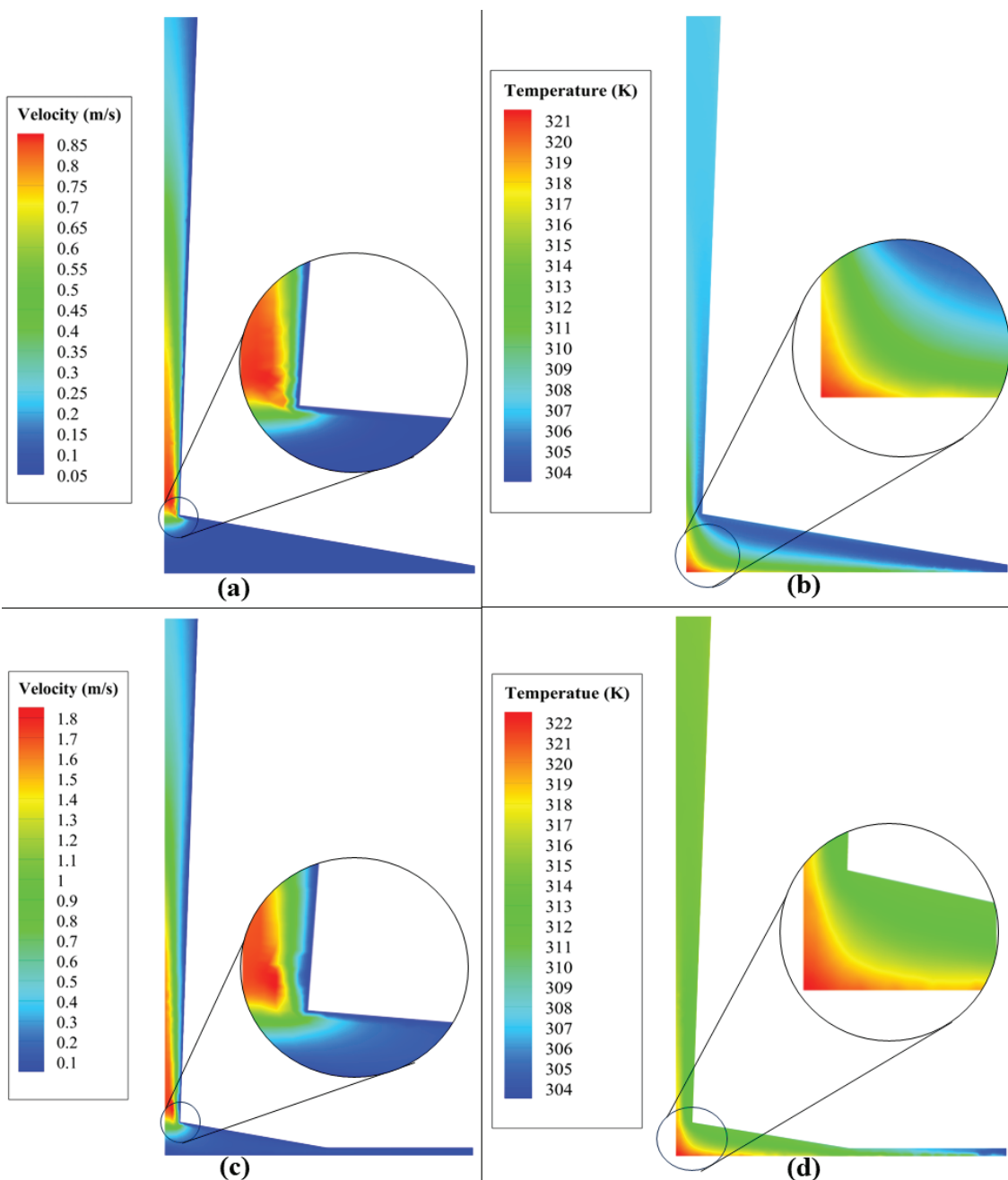


Figure 7. Contour image of, (a) Case 1 - Velocity, (b) Case 1 - Temperature, (c) Case 2 - Velocity, (d) Case 2 – Temperature.

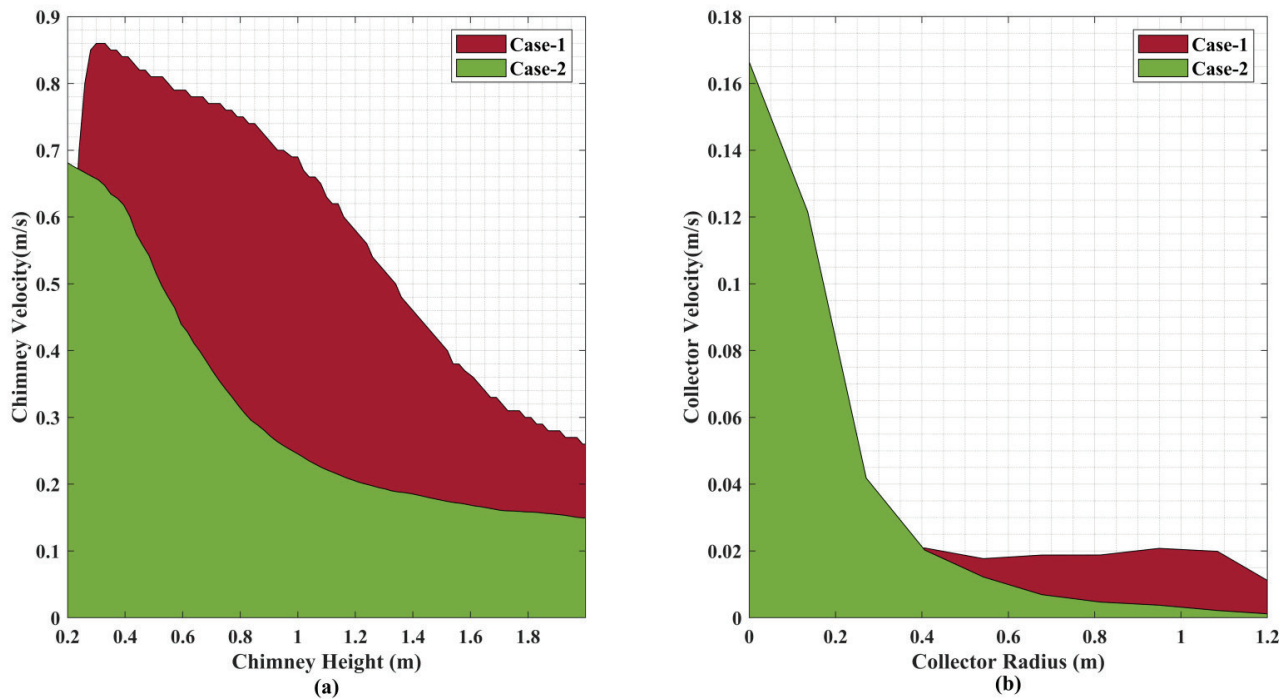


Figure 8. Experiment readings of case-1 and case-2, (a) velocity against chimney height, (b) velocity against collector radius.

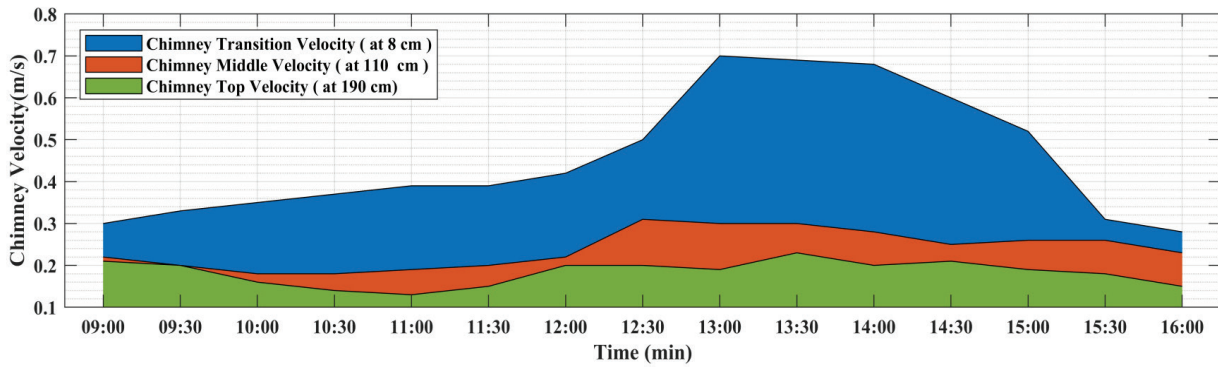
shown in Figures 7b-d demonstrates that the driving potential leads to a density drop, consequently an increase in the temperature of airstream. This Figure 8a and 8b illustrates the change of velocity throughout axis of chimney, collector for case-1 and case-2 respectively. Initially, there is a chimney velocity enhancement at base by narrowing of area, and then gradually decreases as the flow decelerates in divergent section. Notably, there's a steady, slow movement of air at a non-variable flow rate, contributing to a hike in mass flow. However, once the area converges, there's a sudden rush of air into the duct region, leading to a significant spike in velocity. This characteristic stands out as a notable advantage of these models. Upon careful analysis of these findings, it becomes apparent that there are variations in the maximum velocity magnitudes among different cases. Specifically, the increment in collector radius parameter, results an increase in velocity, leads to higher velocity magnitudes.

Figure 9 illustrates velocity, temperature distribution recorded from experimentation of Case 1 and Case 2. These findings reveal the presence of a slump zone at the base of the chimney in both layouts. Additionally, a zone of compression is observed in collector, chimney outlet. Here, Case 1 and Case 2 has a distinct feature in variation of inhabited area of the slump zone (Figure 9a and 9e). The gradient between the collector outlet and inlet is significant in both cases (Figure 9b, 9f). In all scenarios, the temperature beneath the collector increases by approximately 20 K (Figure 9c, 9d, 9g, and 9h). This temperature rise beneath

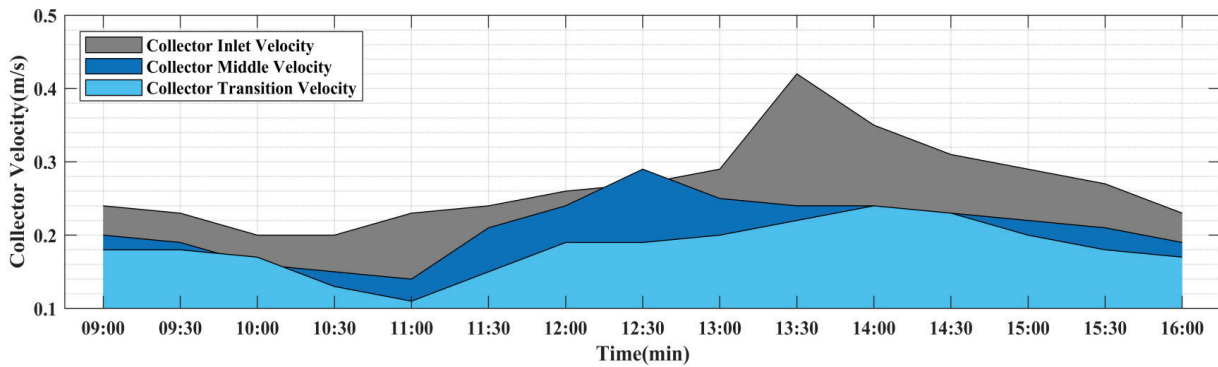
the collector profile is attributed to the lowest air volume. Temperature reduction is enhanced up to ambient conditions on the collector profile from center to inlet location. This temperature differential is crucial for enhancing the collector efficiency. Furthermore, due to the adiabatic design of the chimney and its low height, the airflow in the chimney zone remains warm.

The velocity contour of the case-3 shown in figure has given the following observations. The horizontal movement of air stream inside the vertical chimney is considerably higher at the inlet rather than any section. As it approaches the end of vertical chimney, due to the presence of expansion in chimney profile, there is a reduction in velocity in the divergent section. However, the air stream gains momentum and picks up the energy due to enlargement of air passage. The velocity reaches its peak value of 0.6m/s (Figure 10), but found to be least among other cases considered in this research.

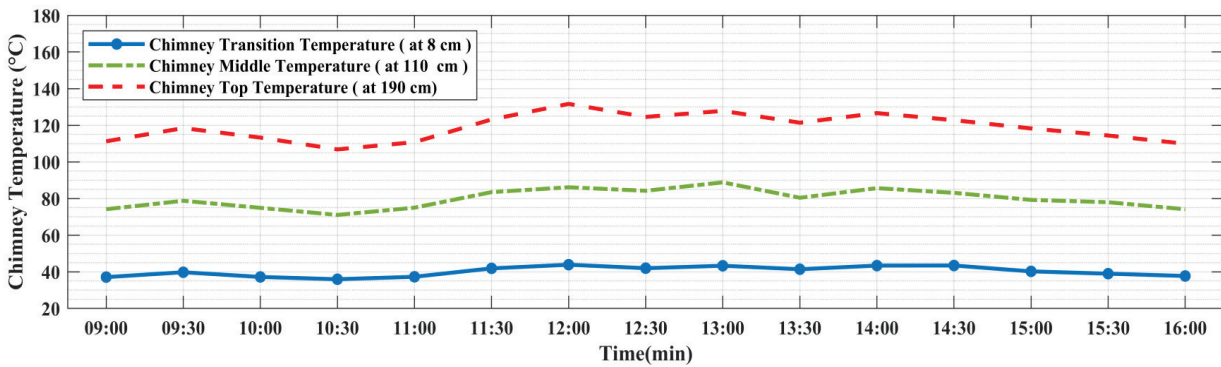
The temperature inside the power plant has an effect of increment in a direction away from collector inlet to chimney inlet sections. Collector walls has a temperature equivalent to ambient conditions mentioned in boundary conditions. Temperature increment from these walls to the ground is visualized in Figure 11. Magnitude of 319 K is achieved at the region closer to the ground, this is referred as the maximum temperature with an increment of 16 K. Further reduction in the temperature along the chimney axial line is achieved in the chimney region. Upward air flow is generated from this location to top



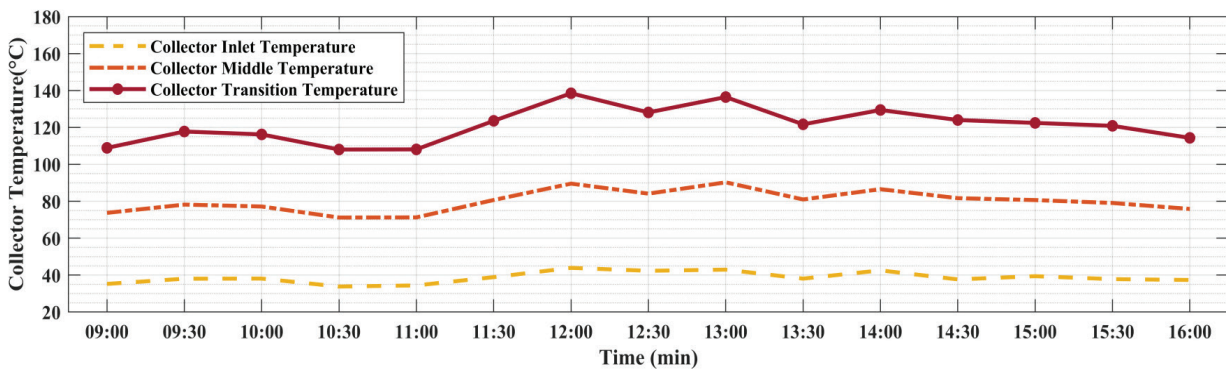
(a)



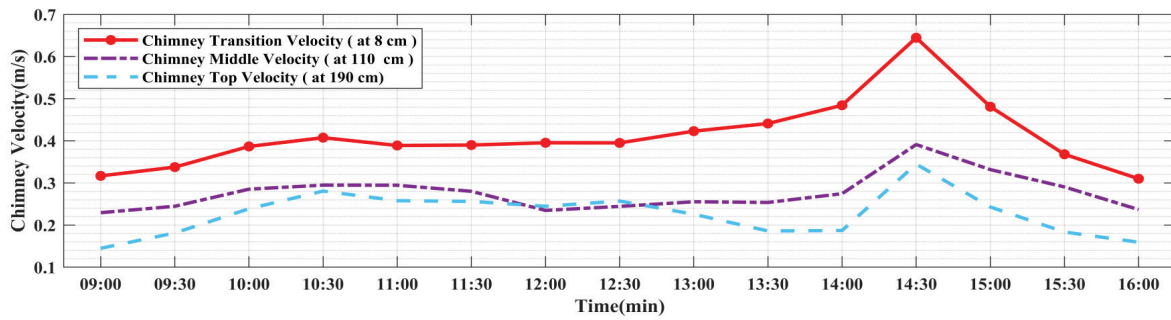
(b)



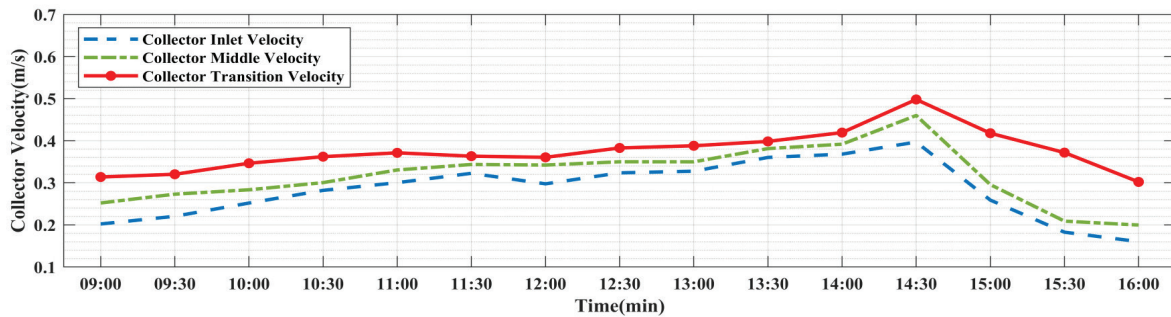
(c)



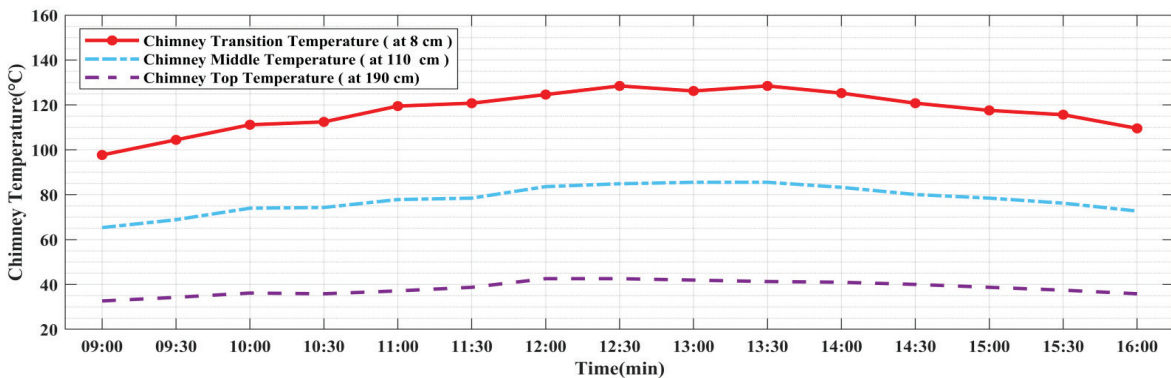
(d)



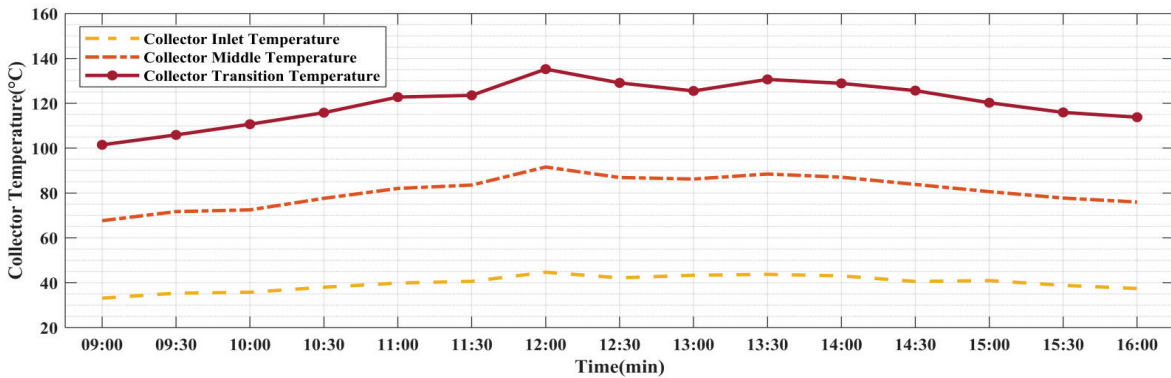
(e)



(f)



(g)



(h)

Figure 9. a) Variation of velocity along the chimney with time (experiment: case-1), b) Velocity variation along collector with time (experiment: case-1), c) Temperature variation along the chimney under time interval (experiment: case-1), d) Temperature variation along the collector under time interval (experiment: case-1), e) Velocity variation across chimney axis with time (experiment: case-2), f) Variation of velocity along the collector with respect to time (experiment: case-2), g) Variation of temperature along the chimney with time (experiment: case-2), h) Variation of temperature along the collector with time (experiment: case-2).

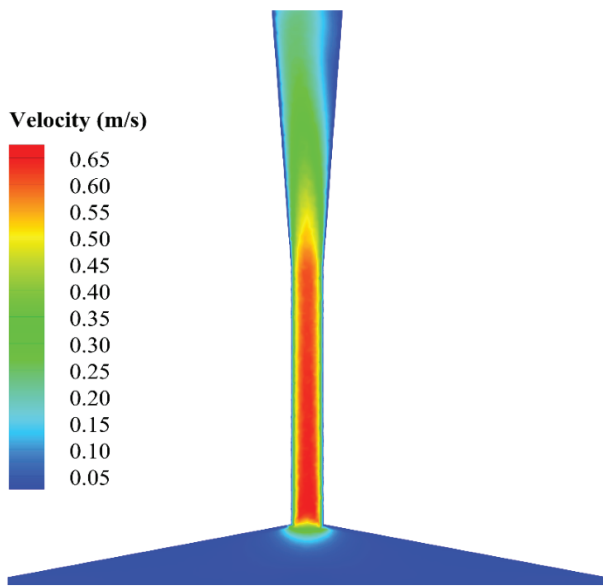


Figure 10. Representation of velocity contour (case-3).

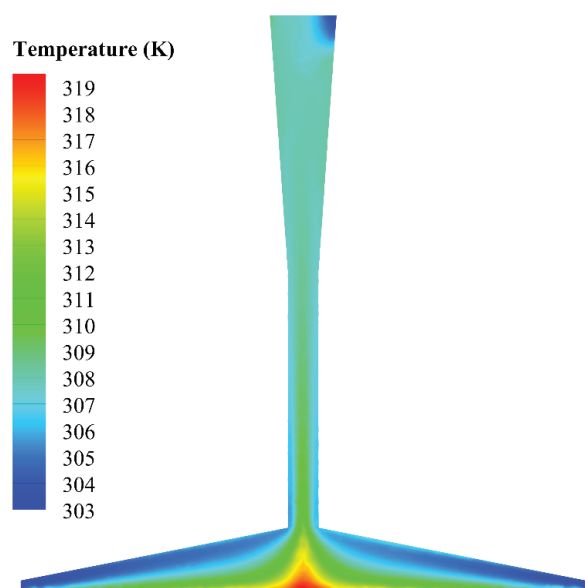


Figure 11. Representation of temperature contour (case-3).

end with maximum velocity magnitude of 0.65 m/s at straight section of chimney, where a minimum of 0.05 m/s is achieved in collector, walls of divergent chimney section.

These experimental results are compared with the computational studies. This resultant plot in this comparison is represented in Figure 12. The model and experimental prototype appear to be in good accord.

Numerical Validation

Magnitude of velocity of all-divergent chimney base sections were included into consideration for this study, clearly demonstrates the impact of area ratio. The case 2 peak magnitude velocity equates to 1.8m/s, temperature increment found to be 18K. Case-1 peak velocity magnitude equals to 0.85m/s. This is 12% inferior to second case and outperformed Manzanares plant by 23%. The case-3 has weaker performance as compared to other cases. The overall

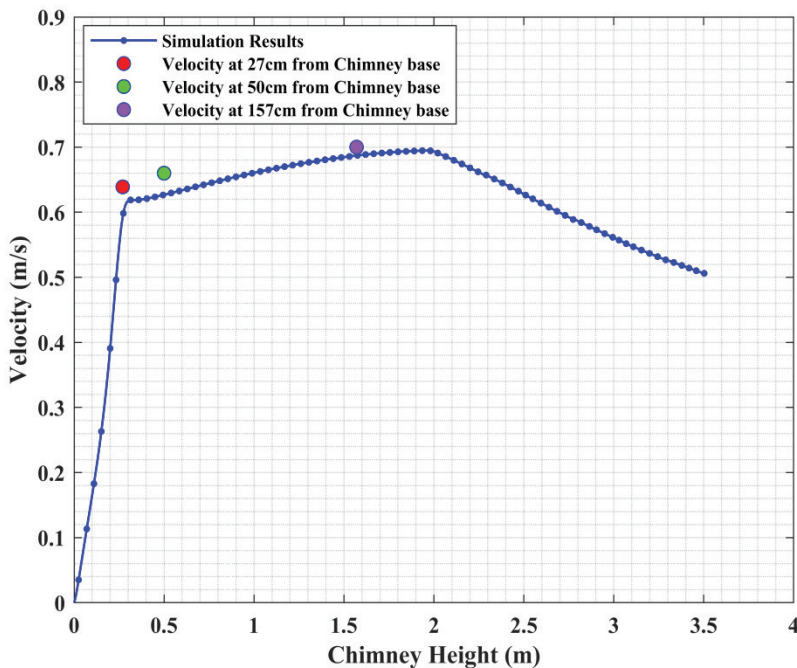


Figure 12. Computational and Experimental results of case-3.

performance is lowered by 23% compared to case-1 and by 12% with case-2. Therefore, case-2 can be an efficient model in terms of higher power generation. Case-1 data is validated with simulation results of [1] by plotting the dimensionless velocity (V/V_{max}), against the dimensionless chimney radius (r/R_o). Here, V is velocity across collector radius, V_{max} is maximum velocity. r is the radial position in collector, R_o is the chimney radius. This validation is carried at a section across the chimney bottom just above the transition region.

The resultant conclusion from this validation expresses better agreement in between both the present numerical results, data from [1], represented in Figure 13. Therefore, maximum velocity is employed at a location closer to chimney bottom, minimum at chimney top.

Figure 14 visualizes chimney velocity variation across r/R_o values in case-3. It was observed the average velocity at chimney base is maximum and there is a gradual reduction

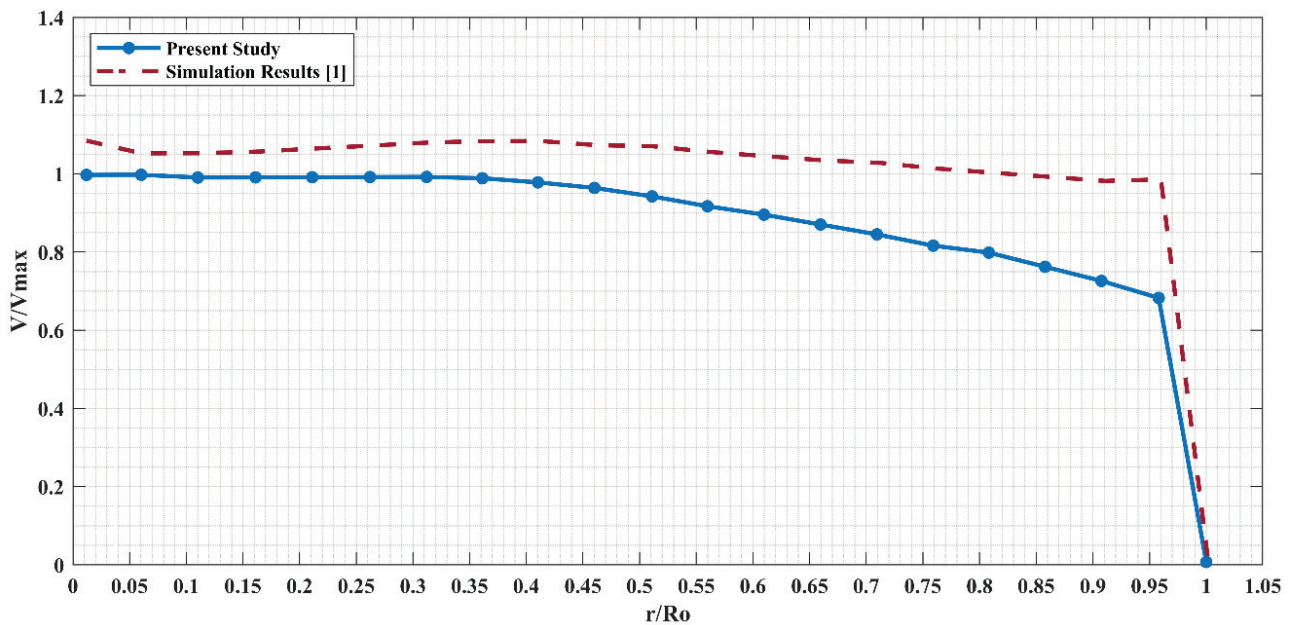


Figure 13. Validation of case 1 with existing study [1].

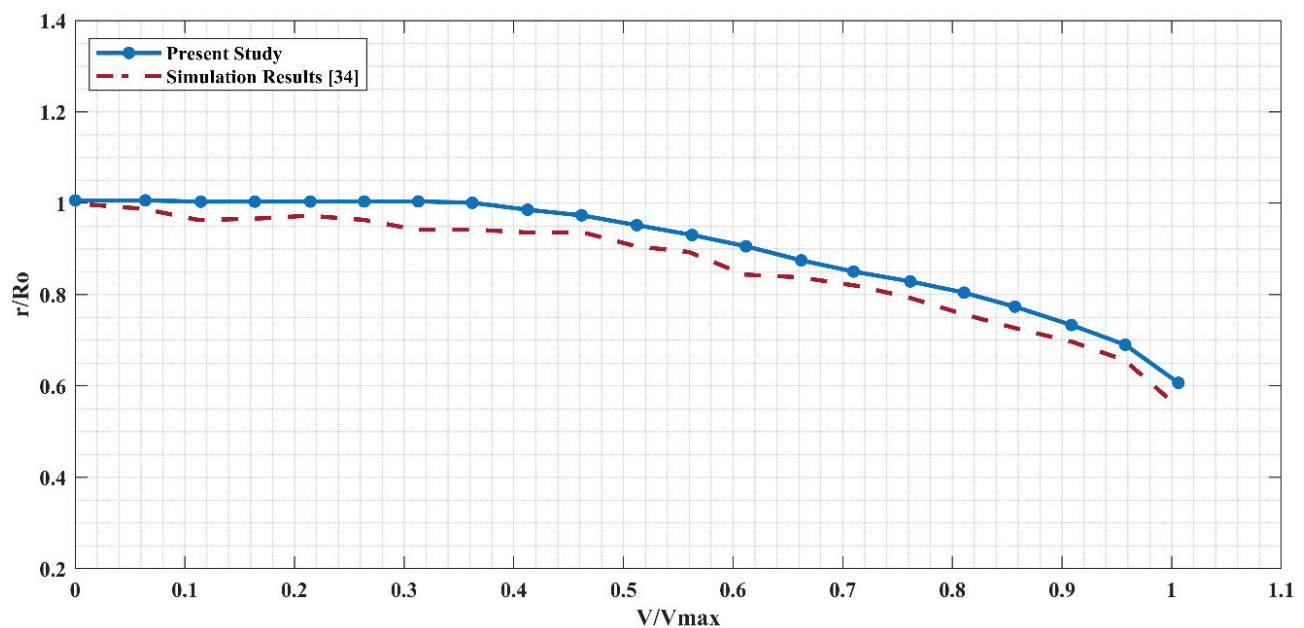


Figure 14. Validation of case-3 simulation results with existing study [34].

towards top section. This validation is to be in close agreement with the study [34].

Environmental Assessment of the Proposed Study

To demonstrate the environmental advantages of utilizing SCPP's, there is necessity for the comparison these to other conventional and emerging power generation systems. One key advantage of SCPP is the lack of water consumption and carbon dioxide production. Hence, a comparison of the daily average rates of CO₂ emissions, water consumption from other power plants within same range in power output similar to this system can demonstrate the environmental advantages of these technologies. Shale gas power plants emit CO₂ and other greenhouse gases during the extraction, transportation, and combustion of shale gas. According to the US Energy Information Administration, shale gas power plants emit an average of 0.82 pounds of CO₂ per kilowatt-hour (kWh) of generated electricity. Figure 15 and 16 compares solar chimney to shale gas power plant and visualizes CO₂ emission and water consumption of two systems along with some known power production units. From this comparison, SCPP is a more ecological friendly alternative to conventional power production systems in terms of these aspects. From Figure 15, and 16, SCPP has dramatically lower water usage and carbon dioxide emissions by 1780.02 and 942.56 kg per day, respectively. It highlights the importance of these systems among the present coal power stations with their high carbon dioxide emissions. In contrast, solar chimney power plants (SCPP) offer a more sustainable solution, as they are capable of reducing CO₂ emissions by 533.6 kg per day when compared to coal power plants of equivalent output power. Additionally, the typical SCPP consumes significantly less

water than coal power plants, highlighting their advantage as an eco-friendly energy source.

Although hydroelectric power plant is considered as eco-friendly in terms of carbon dioxide emissions, it has significant challenge in water-scarce regions due to the higher water consumption. This highlights a major disadvantage of hydroelectric power plants, considered when verifying the feasibility of an appropriate power generation systems for dry regions. Solar chimney power plants (SCPP) offer a significant reduction in water consumption, with the optimized SCPP configuration capable of saving up to 30116.38 kg of water per day. This emphasizes the advantage of SCPP as an environmentally-friendly and sustainable alternative to traditional power generation systems, particularly in areas facing water scarcity issues. Hydroelectric power plants and biomass-derived power plants are both recognized for their high-water consumption rates. Nevertheless, they do not produce significant greenhouse gases. In comparison, typical solar chimney power plants (SCPP) considerably reduce water consumption, with a daily reduction of 13058.5 kg. By implementing the optimal configuration, the reduction rate of water consumption can increase by nearly 200%, reaching up to 41452.32 kg per day. Such a significant reduction of water consumption, particularly in industrial scale, leads to a better remarkable impact around surroundings, particularly in dry regions.

SCPP offers more sustainable and environmentally-friendly solution to traditional power generation systems. In comparison to coal power plants of equivalent output power, A typical SCPP uses a lot less water, mitigates CO₂ emission by 533.6 kg daily. Moreover, revised SCPP arrangement decreases water consumption by 1780.02 kg

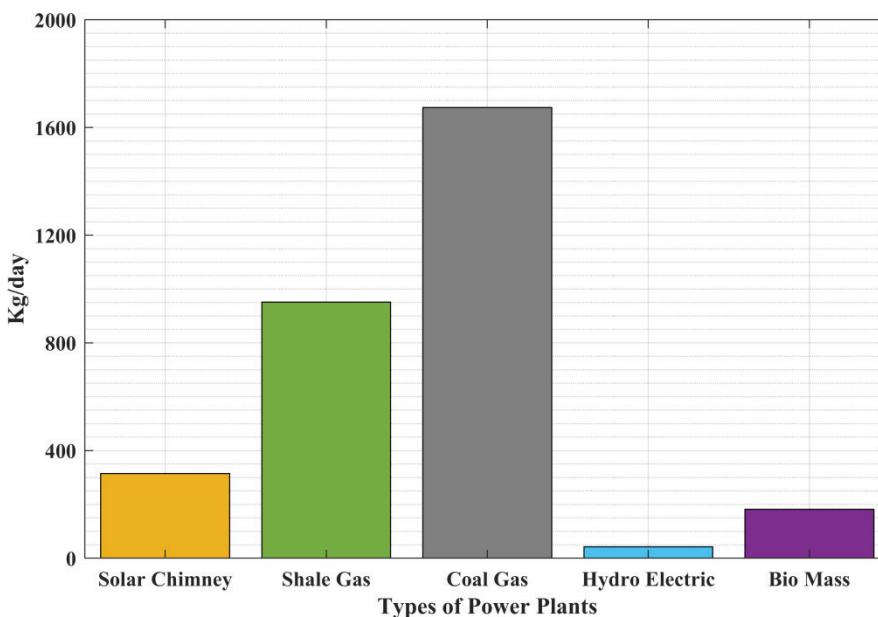


Figure 15. Comparison of SCPP CO₂ emission with conventional power systems.

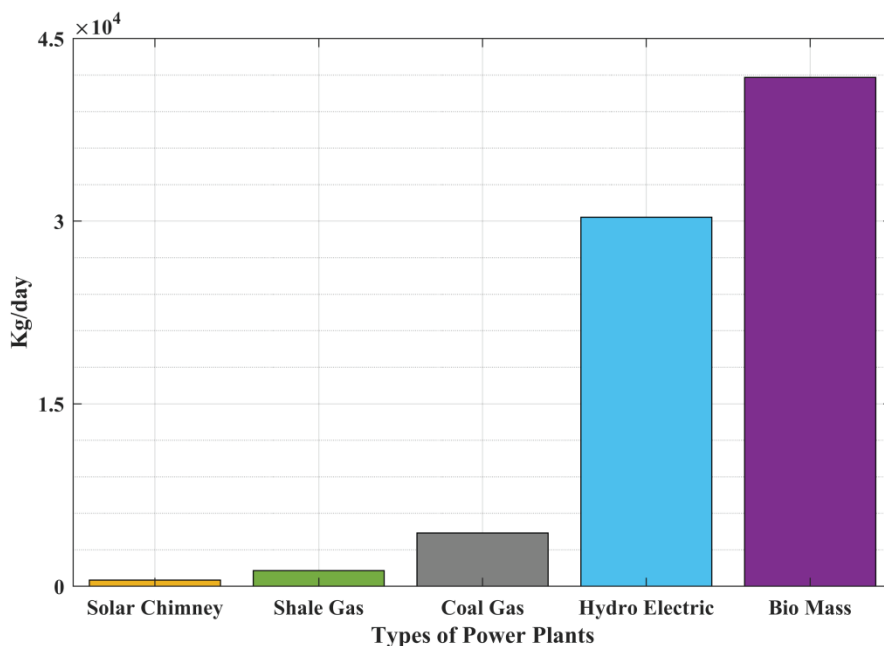


Figure 16. Comparison of SCPP water consumption with conventional power systems.

daily and carbon dioxide emissions by 942.56 kg. The average SCPP uses 13058.5 kg less water per day than hydroelectric power plants and biomass-derived power plants, both of which have high water consumption rates. If the ideal SCPP setup is used, this reduced rate might rise by 200%, to as much as 41452.32 kg per day. Such a significant reduction in water consumption resulted in a remarkable highly positive impact on present circumstances, particularly in dry regions. Therefore, these findings highlight the potential of SCPP as a sustainable and effective alternative to traditional power generation systems, offering significant environmental benefits in terms of greenhouse gas emissions and higher water consumption. SCPP has significant advantages over traditional power generation systems, such as coal power plants, in terms of reducing carbon dioxide emissions. As discussed earlier, typical SCPP can reduce CO₂ emission by 533.6 kg per day, and optimized SCPP configuration can further reduce it by 942.56 kg per day. Therefore, the implementation of SCPP can significantly contribute to reduction of carbon dioxide emissions and provides a better aid to achieve the greenhouse gas reduction standards proposed by the Paris Agreement.

CONCLUSION

Therefore, in an aspect to advance the power output in a same manner of reducing investment costs, it is important to optimize SCPP technologically. This study focused mainly on effects of solar chimney area ratio specifically with diverging chimney equipped with a sloped collector. This research investigates about impact of chimney

expansion on regional airflow characteristics, analyzing variables such as maximum velocity, temperature enhancement for every scenario.

These results demonstrate that the completely divergent chimney significantly increases power output compared to other systems. The advancement of sustainable power production unit based on renewable energy principles is crucial in mitigating environmental risks associated with global warming. SCPP systems offers a prominent solution as an eco-friendly alternative to conventional power generation systems. The evaluation of feasibility of various collector configurations and chimney designs to optimize the SCPP performance through flow parameters is conducted, the results achieved under this study are satisfactory. Case-1 obtained a velocity of 0.85m/s, 12% inferior to second case, here peak magnitude is equivalent to 1.8m/s, with 18 K rise in temperature. The final case performance is 12% less than case-1, 23% lesser than case-2 with 0.6 m/s maximum velocity, 16 K temperature rise. It is concluded that, configuration with completely sloped collector and Semi Divergent (S-D) chimney with a fully sloped collector outperformed another configuration with a 50% sloped collector. SCPP offers significant advantages in terms of reducing water consumption and greenhouse gas emissions compared to conventional and emerging power generation systems. when compared to shale gas power plants, where the emission is 0.82 pounds of CO₂ per kilowatt-hour, the optimized SCPP configuration can reduce carbon dioxide emissions by 942.56 kg per day. Moreover, SCPP greatly reduces water consumption, with optimal configurations

saving up to 41452.32 kg of water per day compared to hydroelectric and biomass-derived power plants.

In future research, the collector configurations can be further studied using different heat storage materials while maintaining the same chimney configuration. Overall, SCPP offers a sustainable and environmentally-friendly solution for power generation, particularly in regions facing water scarcity.

NOMENCLATURE

SCPP	Solar Chimney Power Plant
S-D	Semi Divergent
SUT	Solar Updraft Tower
CFD	Computation Fluid Dynamics

Symbols

β	Slope of the system ($^{\circ}$)
q_{solar}	Solar heat flux (W/m^2)
η_{Coll}	Collector Efficiency (%)
η_{tur}	Turbine Efficiency (%)
η_{tower}	Tower Efficiency (%)
η	Efficiency (%)
P	Electrical power (W)
ΔP	Change in Power (W)
T	Temperature ($^{\circ}\text{C}$)
ρ_{atm}	Density (kg/m^3)
\dot{m}	Mass flow rate (kg/s)
ΔT	Change in temperature ($^{\circ}$)
G	Solar Irradiation (W/m^2)
A	Area of PV (m^2)
A_{coll}	Collector Area (m^2)
Q	Heat (kJ)
p	Pressure (Pa)
Δp	Pressure difference (Pa)
N	Speed of the compressor
C_p	Specific heat capacity at constant pressure ($\text{J}/\text{Kg K}$)
V	Velocity (m/s)
g	Acceleration due to gravity (m/s^2)
r	Radius of the collector
R	Radius of the chimney
r/R_0	Dimensionless chimney radius (Ratio of chimney bottom radius to its outer radius at top)
π	3.14

Subscript

tow	Tower
coll	Collector
tur	Turbine
max	Maximum
min	Minimum
in	Inlet
out	Outlet
atm	Atmospheric condition

AUTHORSHIP CONTRIBUTIONS

All authors contributed to the study conception and design. Methodology, Material preparation and data collection were performed by [Rajamurugu Natarajan], [Akhil Chandramohanan Kumari Suni] The first original draft of the manuscript was written by [Rajamurugu Natarajan], Computational Studies carried out by [Likhith Raj Pedasingu and S.Yaknesh].

DATA AVAILABILITY STATEMENT

All relevant data are within the paper and no additional data are available.

CONFLICT OF INTEREST

The authors declare that they have no known competing financial interests or personal relationships that could have appeared to influence the work reported in this paper.

ETHICS

Not applicable.

REFERENCES

- [1] Das P, Chandramohan V. A critical review on solar chimney power plant technology: influence of environment and geometrical parameters, barriers for commercialization, opportunities, and carbon emission mitigation. *Environ Sci Poll Res* 2022;29:69367-69387. [\[CrossRef\]](#)
- [2] Vakili M, Salehi SA. A review of recent developments in the application of machine learning in solar thermal collector modelling. *Environ Sci Poll Res* 2022;30:2406-2439. [\[CrossRef\]](#)
- [3] Mehta P, Bhatt N, Bassan G, Kabeel AE. Performance improvement and advancement studies of mixed-mode solar thermal dryers: A review. *Environ Sci Poll Res* 2022;29:62822-62838. [\[CrossRef\]](#)
- [4] Purnachandrakumar D, Mittal G, Sharma RK, Singh DB, Tiwari S, Sinhmar H. Review on performance assessment of solar stills using computational fluid dynamics (CFD). *Environ Sci Poll Res* 2022;29:38673-38714. [\[CrossRef\]](#)
- [5] Mehranfar S, Ghareghani A, Azizi A, Mahmoudzadeh Andwari A, Pesyridis A, Jouhara H. Comparative assessment of innovative methods to improve solar chimney power plant efficiency. *Sustain Energy Tech Assess* 2022;49:101807. [\[CrossRef\]](#)
- [6] Das P, Chandramohan V. CFD analysis on flow and performance parameters estimation of solar updraft tower (SUT) plant varying its geometrical configurations. *Energ Source Part A* 2018;40:1532-1546. [\[CrossRef\]](#)

- [7] Das P, Chandramohan VP. Estimation of flow parameters and power potential of solar vortex engine (SVE) by varying its geometrical configurations: A numerical study. *Energy Conver Manage* 2020;223:113272. [\[CrossRef\]](#)
- [8] Gholamalizadeh E, Kim MH. Three-dimensional CFD analysis for simulating the greenhouse effect in solar chimney power plants using a two-band radiation model. *Renew Energy* 2014;63:498-506. [\[CrossRef\]](#)
- [9] Hooi LB, Thangavelu SK. A parametric simulation of solar chimney power plant. *IOP Conf Ser Mater Sci Engineer* 2018;297:012057. [\[CrossRef\]](#)
- [10] Amudam Y, Chandramohan VP. Influence of thermal energy storage system on flow and performance parameters of solar updraft tower power plant: A three dimensional numerical analysis. *J Clean Prod* 2018;207:136-152. [\[CrossRef\]](#)
- [11] Balijepalli R, Chandramohan VP, Kirankumar K, Suresh S. Numerical analysis on flow and performance characteristics of a small-scale solar updraft tower (SUT) with horizontal absorber plate and collector glass. *J Therm Anal Calorim* 2020;141:2463-2474. [\[CrossRef\]](#)
- [12] Chitsomboon T. A validated analytical model for flow in solar chimney. *Int Renew Energy Engineer* 2001;3:339-346.
- [13] Koonsrisuk A. Comparison of conventional solar chimney power plants and sloped solar chimney power plants using second law analysis. *Sol Energy* 2013;98:78-84. [\[CrossRef\]](#)
- [14] Koonsrisuk A. Mathematical modeling of sloped solar chimney power plants. *Energy* 2012;47:582-589. [\[CrossRef\]](#)
- [15] Koonsrisuk A, Chitsomboon T. Effects of flow area changes on the potential of solar chimney power plants. *Energy* 2013;51:400-406. [\[CrossRef\]](#)
- [16] Koonsrisuk A, Chitsomboon T. A single dimensionless variable for solar chimney power plant modeling. *Sol Energy* 2009;83:2136-2143. [\[CrossRef\]](#)
- [17] Koonsrisuk A, Chitsomboon T. Mathematical modeling of solar chimney power plants. *Energy* 2013;51:314-322. [\[CrossRef\]](#)
- [18] Ayadi A, Driss Z, Bouabidi A, Abid MS. Effect of the number of turbine blades on the air flow within a solar chimney power plant. *Proc Inst Mech Engineer A: J Power Energy* 2017;232:425-436. [\[CrossRef\]](#)
- [19] Cao F, Zhao L, Li H, Guo L. Performance analysis of conventional and sloped solar chimney power plants in China. *Appl Therm Engineer* 2012;50:582-592. [\[CrossRef\]](#)
- [20] Koonsrisuk A, Lorente S, Bejan A. Constructural solar chimney configuration. *Int J Heat Mass Transf* 2010;53:327-333. [\[CrossRef\]](#)
- [21] Zhou X, Yang J, Xiao B, Hou G, Wu Y. Numerical investigation of a compressible flow through a solar chimney. *Heat Transf Engineer* 2009;30:670-676. [\[CrossRef\]](#)
- [22] Ming T, Liu W, Pan Y, Xu G. Numerical analysis of flow and heat transfer characteristics in solar chimney power plants with energy storage layer. *Energy Conver Manage* 2008;49:2872-2879. [\[CrossRef\]](#)
- [23] Keshari SR, Chandramohan VP, Das P. A 3D numerical study to evaluate optimum collector inclination angle of Manzanares solar updraft tower power plant. *Sol Energy* 2021;226:455-467. [\[CrossRef\]](#)
- [24] Sundararaj M, Rajamurugu N, Anbarasi J, Yaknesh S, Sathyamurthy R. Parametric optimization of novel solar chimney power plant using response surface methodology. *Results Engineer* 2022;16:100633. [\[CrossRef\]](#)
- [25] Ghalamchi M, Kasaeian A, Ghalamchi M. Experimental study of geometrical and climate effects on the performance of a small solar chimney. *Renew Sustain Energy Rev* 2015;43:425-431. [\[CrossRef\]](#)
- [26] Gannon AJ, von Backstrom TW. Solar chimney cycle analysis with system loss and solar collector performance. *J Sol Energy Engineer* 2000;122:133-137. [\[CrossRef\]](#)
- [27] Guo HJ, Li JL, Huang SH. Heat storage performance analysis of solar chimney power plant system. *Appl Mech Mater* 2014;472:276-285. [\[CrossRef\]](#)
- [28] Koonsrisuk A, Chitsomboon T. Accuracy of theoretical models in the prediction of solar chimney performance. *Sol Energy* 2009;83:1764-1771. [\[CrossRef\]](#)
- [29] Mehdipour R, Habibi M, Eydiyan M, Mohammadi E, Baniamerian Z. Experimental assessment of energy tower's performance: Evaluation of the impacts of solar radiation, humidity, and chimney's height on the overall efficiency. *Environ Sci Poll Res* 2024;31:18200-18208. [\[CrossRef\]](#)
- [30] Ridwan A, Hafizh H, Fauzi MR. Design and experimental test for solar chimney power plant: Case study in Riau Province, Indonesia. *IOP Conf Ser Mater Sci Engineer* 2018;403:012092. [\[CrossRef\]](#)
- [31] Okada S, Uchida T, Karasudani T, Ohya Y. Improvement in solar chimney power generation by using a diffuser tower. *J Sol Energy Engineer* 2015;137:031009. [\[CrossRef\]](#)
- [32] Natarajan R, Jayaraman V, Sathyamurthy R. Comparative studies on performance of solar towers with variable scale ratios. *Environ Sci Poll Res* 2022;29:45601-45611. [\[CrossRef\]](#)
- [33] Zhou XP, Yang JK. Temperature field of solar collector and application potential of solar chimney power systems in China. *J Energy Inst* 2008;81:25-30. [\[CrossRef\]](#)
- [34] Zhou X, Yang J, Xiao B, Hou G. Experimental study of temperature field in a solar chimney power setup. *Appl Therm Engineer* 2007;27:2044-2050. [\[CrossRef\]](#)
- [35] Kassaei F, Ghodsi A, Jadidi A, Valipour MS. Experimental studies on solar chimneys for natural ventilation in domestic applications: A comprehensive review. *Environ Sci Poll Res* 2022;29:73842-73855. [\[CrossRef\]](#)

- [36] Ikhlef K, Ucgul I, Larbi S, Ouchene S. Performance estimation of a solar chimney power plant (SCPP) in several regions of Turkey. *J Therm Engineer* 2022;8:202-220.
- [37] Chitsomboon T. Potential and efficiency of solar chimney in the production of electrical energy. *Res Develop J Engineer Inst Thailand* 2000;11:38-44.
- [38] Ferreira AG, Maia CB, Cortez MF, Valle RM. Technical feasibility assessment of a solar chimney for food drying. *Sol Energy* 2008;82:198-205. [\[CrossRef\]](#)
- [39] Das P, Chandramohan V. 3D numerical study on estimating flow and performance parameters of solar updraft tower (SUT) plant: Impact of divergent angle of chimney, ambient temperature, solar flux and turbine efficiency. *J Clean Prod* 2020;256:120353. [\[CrossRef\]](#)
- [40] Rao TB, Sivalingam M. Assessment of energy, exergy, environmental, and economic study of an evacuated tube solar dryer for drying Krishna Tulsi. *Environ Sci Poll Res* 2023;30:67351-67367. [\[CrossRef\]](#)
- [41] Muthu V, Ramadas G. Experimental investigation of 4E performance studies of a vertical bifacial solar module during summer and winter. *Environ Sci Poll Res* 2022;29:17943-17963. [\[CrossRef\]](#)
- [42] Nazari S, Daghigh R. Techno-enviro-exergo-economic and water hygiene assessment of non-cover box solar still employing parabolic dish concentrator and thermoelectric peltier effect. *Proc Safety Environ Protect* 2022;162:566-582. [\[CrossRef\]](#)
- [43] Sadeghi G, Nazari S. Retrofitting a thermoelectric-based solar still integrated with an evacuated tube collector utilizing an antibacterial-magnetic hybrid nanofluid. *Desalination* 2021;500:114871. [\[CrossRef\]](#)
- [44] Phu NM, Kha NH, Hap NV. Impact of the V CAP on induced turbulent air flow in a solar chimney: A computational study. *J Therm Engineer* 2023;9:510-517. [\[CrossRef\]](#)
- [45] Zhou X, Yang J, Xiao B, Hou G, Xing F. Analysis of chimney height for solar chimney power plant. *Appl Therm Engineer* 2009;29:178-185. [\[CrossRef\]](#)
- [46] Hu S, Leung DYC, Chen MZQ. Effect of divergent chimneys on the performance of a solar chimney power plant. *Energy Proc* 2017;105:7-13. [\[CrossRef\]](#)